



## HIGH PERFORMING ULTRA-DURABLE MEMBRANE ELECTRODE ASSEMBLIES FOR TRUCKS

**Grant agreement no.: 101101346**

**Start date:** 01.01.2023 – **Duration:** 36 months

**Project Coordinator:** D. J. Jones, CNRS

*The HIGHLANDER project is supported by the Clean Hydrogen Partnership and its members Hydrogen Europe and Hydrogen Europe Research.*

*Views and opinions expressed are however those of the author(s) only and do not necessarily reflect those of the European Union or Clean Hydrogen JU. Neither the European Union nor the granting authority can be held responsible for them.*

## DELIVERABLE REPORT

D3.3: MODIFIED SUPPORT DEVELOPED THAT LEADS TO INCREASED CATALYST-SUPPORT AND IONOMER-SUPPORT INTERACTION, AND IMPROVED IONOMER STABILITY IN THE CATHODE CATALYST LAYER		
Due Date		31 December 2024
Author (s)		Lujin Pan, Jiasheng Lu, Fabio Dionigi, Peter Strasser, Sara Cavaliere, Rémi Bacabe, Pierre-Yves Blanchard, Olivia Dunseath, Enrico Petrucco
Workpackage		WP3
Workpackage Leader		TUB
Lead Beneficiary		CNRS
Date released by WP leader		1 April 2025
Date released by Coordinator		1 April 2025
DISSEMINATION LEVEL		
PU	Public	X
SEN	Sensitive, limited under the conditions of the Grant Agreement	
NATURE OF THE DELIVERABLE		
R	Document, report	X
DEM	Prototype demonstrator	

SUMMARY	
<b>Keywords</b>	<i>Sulfur-doped carbon; catalyst-support interaction; ionomer-support interaction; ionomer stability; PtCo intermetallic</i>
<b>Abstract</b>	<i>Work Package 3 (WP3) aims to develop advanced catalysts with optimized synthesis strategies, improved characterization, and enhanced electrochemical performance. The objective is to achieve high activity and stability with minimal PGM loading by ensuring homogeneous ionomer coverage and controlled catalyst deposition. The approach involves modifying carbon supports to promote specific interactions with catalyst nanoparticles and ionomers, improving dispersion and adhesion. Various characterization techniques, including XPS and immersion calorimetry, are used to assess electronic interactions and quantify ionomer affinity. Sulfur-functionalized supports are evaluated for their impact on hydrophilicity, catalyst stability, and electrochemical surface area retention. The role of surface modifications in enhancing catalyst performance is investigated. The methodology integrates material design with performance validation to ensure practical applicability. The findings contribute to developing durable, high-performance catalysts for fuel cell applications.</i>
<b>Public abstract for confidential deliverables</b>	<i>As above</i>

REVISIONS			
Version	Date	Changed by	Comments
0.1	28/02/2025	L. Pan (TUB)	Drafted
0.2	05/03/2025	S. Cavaliere, R. Bacabe (CNRS)	Additions
0.3	27/03/2025	O. Dunseath (JM)	Additions
0.4	30/03/2025	S. Cavaliere (CNRS)	Finalisation

## MODIFIED SUPPORT DEVELOPED THAT LEADS TO INCREASED CATALYST-SUPPORT AND IONOMER SUPPORT INTERACTION, AND IMPROVED IONOMER STABILITY IN THE CATHODE CATALYST LAYER

### CONTENTS

1	Introduction.....	4
2	Experimental .....	4
2.1	Synthesis of sulfur-containing carbon (SC) and PtCo/SC_7 & 11 nm SiO <sub>2</sub> .....	4
2.2	Electrochemical characterisation.....	4
2.3	XPS characterisation .....	5
2.4	Immersion calorimetry.....	5
3	Discussion .....	5
3.1	Catalyst-support interaction .....	5
3.1	Carbon-ionomer interaction strength.....	7
3.2	Improved cathode catalyst layer stability.....	9
4	Conclusions and future work.....	10
5	References.....	11

## 1 INTRODUCTION

Work Package 3 (WP3) focuses on developing advanced catalysts and catalyst supports, specifically aiming to improve synthesis strategies, characterisation and quantification of the interaction within catalyst layer, stability and activity screening by electrochemical measurements and validation in single cell tests.

In order to obtain high active and stable catalyst layers with minimum PGM loading, the homogeneity of the ionomer coverage and of the deposition of nanocatalysts on the carbon support particles is crucial. The approach used in the Highlander project is the preparation of chemically modified carbon supports allowing specific interactions with the PGM nanoparticles as well as with the PFSA ionomer, and therefore a controlled coverage. The role of heteroatom on the support on the ionomer distribution around the catalyst has been highlighted by previous works.<sup>1, 2</sup>

In particular, a range of characterization techniques has been used to investigate and quantify the strength of the interaction of supports functionalized with sulfur (SC) with the Pt-based electrocatalyst and the PFSA ionomer in comparison with a non-modified reference carbon support (C1).

The study of Pt 4f and S 2p signals in X-ray photoelectron spectroscopy (XPS) and their shifts compared to reference electrocatalysts was performed to evidence electronic interactions and compare bond strength between the catalyst, the support and the Nafion ionomer.

Immersion calorimetry was performed to quantify the interaction between ionomer and carbon, and specifically the role of the sulfur functionalisation on the catalyst support on the electrode performance and stability. Calorimetry experiments were already used to characterise the strength of interaction between N-doped carbons and ionomer.<sup>3</sup> The enthalpy of immersion ( $\Delta H_{imm}$ ) in water and in aqueous dispersions of Aquivion of different equivalent weights (EW 980 and 790) were measured. This allowed assessment of the support hydrophilicity as well as the strength of interaction with Aquivion to explain the enhanced ECSA retention observed in *ex situ* electrochemical measurements.

Finally, to assess the ionomer stability in the catalyst layer ORR mass activity and ECSA evolution on PtCo/SC and reference Pt/C1 electrocatalysts were evaluated upon an accelerated stress test (AST).

## 2 EXPERIMENTAL

### 2.1 Synthesis of sulfur-containing carbon (SC) and PtCo/SC\_7 & 11 nm SiO<sub>2</sub>

The synthesis of sulfur-carbon (SC) materials using 7 nm and 11 nm SiO<sub>2</sub> templates involved dissolving 2,2'-bithiophene in THF, followed by the addition of Co(NO<sub>3</sub>)<sub>2</sub>·6H<sub>2</sub>O and SiO<sub>2</sub> templates. After stirring for 4 h, the solvent was evaporated, and the resulting material was ground into a powder and pyrolysed at 800 °C under N<sub>2</sub> for 2 h. The SiO<sub>2</sub> template was removed via alkaline etching in NaOH at 100 °C, followed by acid treatment in H<sub>2</sub>SO<sub>4</sub>, washing, and freeze-drying. The synthesis of 50 % PtCo/SC\_7 & 11 nm SiO<sub>2</sub> catalysts involved dispersing SC in water, introducing a Pt and Co precursor solution, and drying the mixture before annealing at 950 °C for 2 h and then 600 °C for 6 h under 4 % H<sub>2</sub>/Ar. Post-treatment for PtCo/SC\_7 nm SiO<sub>2</sub> included acid leaching in HClO<sub>4</sub> at 60 °C and annealing at 400 °C, while PtCo/SC\_11 nm SiO<sub>2</sub> underwent pre-leaching in H<sub>2</sub>SO<sub>4</sub> at 80 °C for 24 h before the final annealing step.

### 2.2 Electrochemical characterisation

RDE measurement was conducted in a three-electrode half-cell with working electrode (WE) on to which the samples were drop-cast, graphite as counter electrode (CE) and mercury mercurous sulfate (MMS) as

reference electrode. The RDE was done by performing cyclic voltammetry (CV) in  $N_2$  with  $20 \text{ mV s}^{-1}$  from 0.05 to  $0.95 V_{RHE}$  for  $ECSA_{HUPD}$ , linear sweep voltammetry in  $O_2$  with  $20 \text{ mV s}^{-1}$  from 0.05 to  $1.0 V_{RHE}$  for ORR activity and CO-stripping in  $N_2$  after CO poisoning the WE surface with  $50 \text{ mV s}^{-1}$  from 0.05 to  $1.1 V_{RHE}$  for  $ECSA_{CO}$ . The accelerated stress test (AST) consists of 30,000 trapezoidal cycles between  $0.6 V_{RHE}$  and  $0.95 V_{RHE}$ , with a sweeping rate of  $700 \text{ mV s}^{-1}$  and a holding time of 3 seconds, one full cycle is 7 s.

## 2.3 XPS characterisation

X-ray photoelectron spectroscopy (XPS) measurements were performed using a ThermoScientific K Alpha+ X-ray Photoelectron Spectrometer. All samples were analysed using a microfocused, monochromated Al K  $\alpha$  X-ray source (1486.68 eV;  $400 \mu\text{m}$  spot size) while the analyser had a pass energy of 50 eV. To prevent any localized charge buildup during analysis the K-Alpha+ charge compensation system was employed at all measurements. The peak fitting was performed using CasaXPS software.

## 2.4 Immersion calorimetry

The hydrophilic character and the carbon-ionomer interaction strength were evaluated at CNRS using immersion calorimetry for the sulfur doped carbon SC\_11 nm in comparison to non-functionalised carbon blacks: C1 from JM, EC300J Ketjenblack EC300J (KB3) and Vulcan XC72R (V). The ionomers were 25 wt% aqueous dispersions of 980 EW Aquivion and 790 EW Aquivion from Syensqo. 40 mg of sample were dried at  $200^\circ\text{C}$  under vacuum for 12 hours in a glass vial before being sealed under vacuum. The vial was then introduced in a crucible containing either deionised water ( $18.2 \text{ M}\Omega \text{ cm}^2$ ) or aqueous ionomer dispersion, within the thermostated calorimeter. Sample and solution were heated to  $30^\circ\text{C}$ . After temperature equilibration, the vial was broken to put the carbon in contact with the liquid medium and the heat flow on its immersion was measured. The heat flow was integrated over time to access the enthalpy of immersion ( $\Delta H_{imm}$ ) and normalised by the mass or by the specific surface area previously determined using  $N_2$  adsorption-desorption *via* the BET method.

# 3 DISCUSSION

## 3.1 Catalyst-support interaction

To gain deeper insights into the interaction between the supports, nanoparticles and ionomer, XPS measurement was conducted on JM Pt/C1, PtCo/SC\_7 nm and PtCo/SC\_11 nm, with and without Nafion. The figure 1 presents the XPS spectra of Pt-4f. The left panel shows samples without Nafion, the Pt-4f spectra for all three samples show peaks corresponding to Pt(0) and Pt(II) states, shown in dark blue and grey, respectively. Pt(0) is significant because it represents the metallic state of platinum, which is typically the most catalytically active form of Pt in many electrochemical reactions, such as ORR in fuel cells. The lower binding energy of Pt(0)  $4f_{7/2}$  in the both PtCo/SC samples, compared to the Pt/C reference, clearly indicates electron transfer from cobalt or from the support to platinum. This electron transfer modifies the electronic structure of Pt, increasing its electron density and potentially enhancing its catalytic activity.

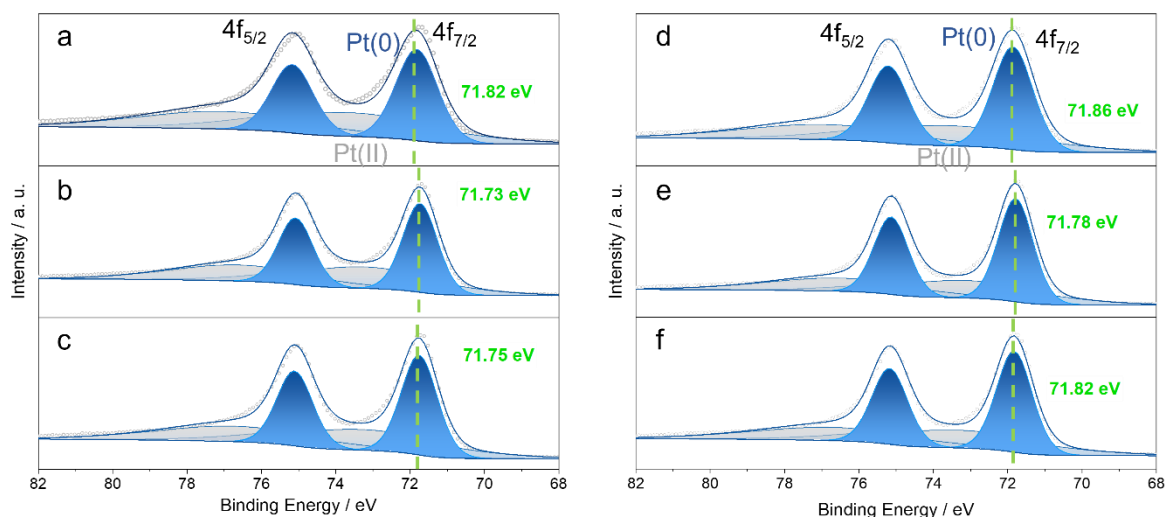


Figure 1: XPS spectra of Pt-4f in samples without Nafion addition (left column) and with Nafion (right column). (a)(d) JM Pt/C1, (b)(e) PtCo/SC\_7 nm, (c)(f) PtCo/SC\_11 nm.

For the JM Pt reference (Figure 1 a, d), the Pt-4f spectra display well-defined peaks with binding energies centred at 71.82 eV (without Nafion) and 71.86 eV (with Nafion). This subtle shift suggests that Nafion introduces an electronic interaction, likely through electrostatic or ligand effects from its sulfonic acid groups. The similar trend is observed for PtCo/SC\_7 nm (Figure 1 b, e) and PtCo/SC\_11 nm (Figure 1 c, f), where the binding energy of Pt(0) increases upon Nafion addition, moving from 71.73 eV to 71.78 eV for PtCo/SC\_7 nm and from 71.75 eV to 71.82 eV for PtCo/SC\_11 nm. Noteworthy is the 70 meV for PtCo/SC\_11 nm was the largest, this might be related to the previously reported large surface area of the support. These shifts indicate that Nafion modifies the local electron density of Pt sites, possibly by withdrawing electron density due to its acidic nature.

The XPS spectra of the S-2p region (Figure 2) provide further understanding into the interaction between Nafion and the catalyst in different samples. In Pt/C1 (Figure 2a), the S-2p peak appears at the highest binding energy (168.87 eV). For PtCo/SC\_7 nm (Figure 2 b) and PtCo/SC\_11 nm (Figure 2 c), the binding energy shifts to lower values (168.68 eV and 168.60 eV, respectively). This shift to lower binding energy suggests a stronger overall interaction between Nafion and the PtCo/SC catalysts. The presence of cobalt and sulfur on the support likely modifies the electronic environment, enhancing the interaction with Nafion. Cobalt can donate electrons, increasing electron density around the sulfur atoms in Nafion, while sulfur on the support may further contribute to this effect. This stronger interaction is crucial for improving proton conduction and catalyst stability in fuel cell applications.

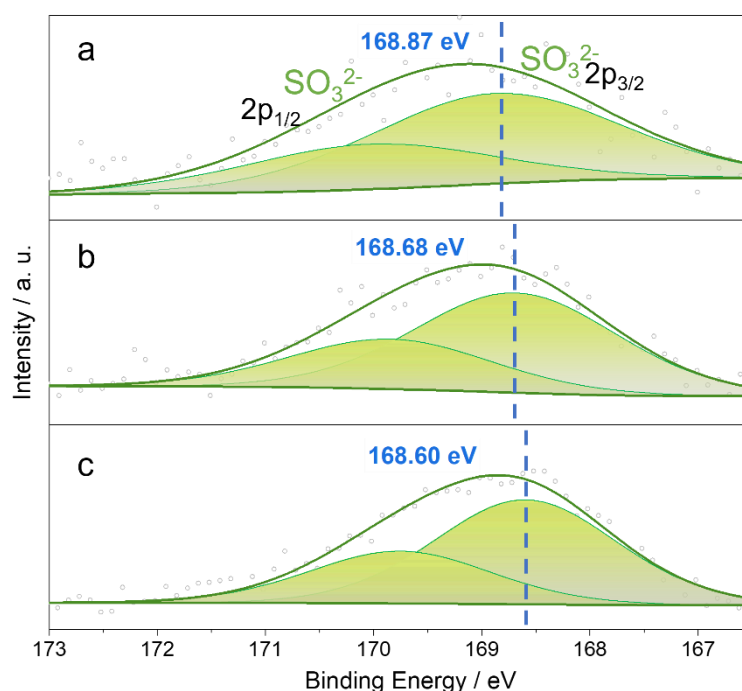


Figure 2: XPS spectra of S-2p in samples with Nafion, (a) JM Pt/C1, (b) PtCo/SC\_7 nm, (c) PtCo/SC\_11 nm.

The XPS data reveal that PtCo/SC samples exhibit enhanced electronic interactions and stronger Nafion binding compared to JM Pt/C1. The lower Pt(0) binding energy indicates electron transfer from cobalt or the support, increasing Pt's electron density. The reduced S-2p binding energy in PtCo/SC samples suggests stronger Nafion-catalyst interactions.

### 3.1 Carbon-ionomer interaction strength

The first part of the work entailed the investigation of the interaction of carbon blacks with water to assess their hydrophilic properties, which can be modified by the presence of the heteroatom in the carbon structure. The various carbon supports were immersed in water, and heat flow was recorded. The integration of the peak as a function of the time gave access to the immersion enthalpy, which was normalised either by the mass of carbon sample or the specific surface area of the carbon (Table 1). In Figure 3 are presented the obtained immersion enthalpy values.

Table 1. Specific surface area and pore surface and volume for the investigated carbon blacks.

Sample	S <sub>BET</sub> (m <sup>2</sup> ·g <sup>-1</sup> )	S <sub>NL-DFT</sub> (m <sup>2</sup> ·g <sup>-1</sup> )	S <sub>micropores</sub> (m <sup>2</sup> ·g <sup>-1</sup> )	S <sub>mesopores</sub> (m <sup>2</sup> ·g <sup>-1</sup> )	V <sub>NL-DFT</sub> (cm <sup>3</sup> ·g <sup>-1</sup> )	V <sub>micropores</sub> (cm <sup>3</sup> ·g <sup>-1</sup> )	V <sub>mesopores</sub> (cm <sup>3</sup> ·g <sup>-1</sup> )
KB3 EC300J (KB3)	800	784	571	213	1.204	0.259	0.945
Vulcan XC72-R (V)	230	239	188	51	0.284	0.091	0.193
SC-11nm	1345						
C1	783						



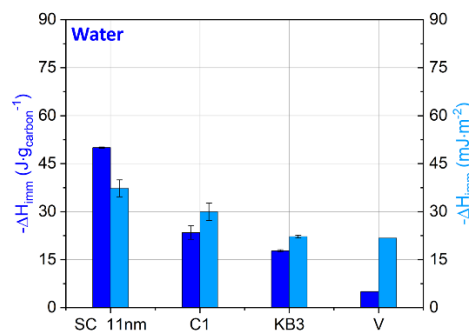


Figure 3: Immersion enthalpy for the different carbon supports in deionised water.

The contact between water and carbon induces an exothermic heat flow. Carbon blacks show different mass-normalised  $\Delta H_{imm}$  principally due to the difference in specific surface area (230 m<sup>2</sup> g<sup>-1</sup> for Vulcan XC72-R (V); 800 m<sup>2</sup> g<sup>-1</sup> for KB3; 780 m<sup>2</sup> g<sup>-1</sup> for C1 and 1345 m<sup>2</sup> g<sup>-1</sup> for SC\_11 nm). Immersion enthalpies increase with increased surface area of the supports, with highest value for SC\_11 nm.

To decorrelate the effect of the surface area on the immersion enthalpy, the values were normalised by the BET surface area. V and KB3 show  $\Delta H_{imm}$  around 22 mJ m<sup>-2</sup> whereas C1 reached a  $\Delta H_{imm}$  of 29.9 mJ m<sup>-2</sup> and SC\_11 NM 37 mJ m<sup>-2</sup>. SC\_11 NM presents a higher surface area normalised  $\Delta H_{imm}$  than the other carbon blacks, indicating a higher hydrophilicity which can be correlated to the presence of sulfur. These results are in accordance with the bibliography where the presence of heteroatoms on the carbon surface enhances its hydrophilic character, leading to higher wettability.<sup>4</sup>

Immersion calorimetry on the different carbon was conducted using a 25wt% Aquivion 980 EW dispersed in water, the results are shown in Figure 4.

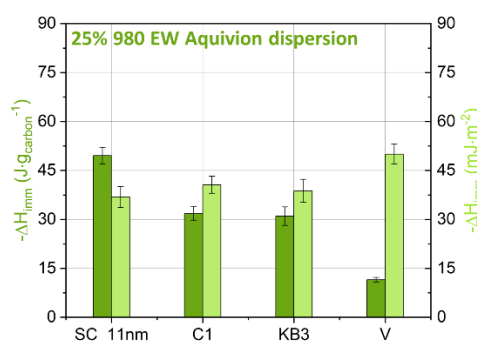


Figure 4. Immersion enthalpy for the different carbon supports in 25 wt% 980 EW Aquivion dispersion.

The heat flow when SC\_11 nm is immersed in aqueous Aquivion ionomer dispersion is almost identical to that which occurs when it is immersed in water. This observation is different from that with the other carbons, where the heat flow is higher in Aquivion than in water, indicating an interaction between the carbon surface and the ionomer. When  $\Delta H_{imm}$  is normalised by the mass of carbon sample, Vulcan show the lowest  $\Delta H_{imm}$  with 11.5 J g<sup>-1</sup> and SC\_11 nm the highest (49.6 J g<sup>-1</sup>), which can be explained by their



respectively lowest and highest specific surface area. When normalised by the specific surface area of carbon sample, the enthalpy of immersion is similar for all the samples, although is higher for Vulcan XC72.

The same experiment was performed using 25 wt% 790 EW Aquivion dispersion (Figure 5).

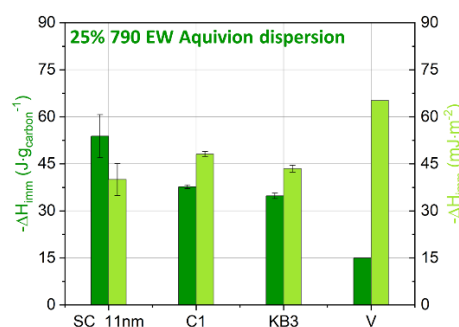


Figure 5. a) Immersion enthalpy for the different carbon support in 25wt% 790 EW Aquivion dispersion.

A similar trend is observed with 790 EW Aquivion, but the enthalpy of immersion is higher than with 980 EW Aquivion. This result suggests that the interaction between ionomer and support takes place preferentially *via* the SO<sub>3</sub>H groups of the ionomer, which are more highly concentrated in 790 EW Aquivion. However, in general, the enthalpy of immersion of SC\_11 nm is similar in water and in the two Aquivion aqueous dispersions, while it is higher in Aquivion dispersion than in water for the three other carbons. Based on calorimetry measurements therefore, SC\_11 nm does not seem to promote increased interaction with Aquivion dispersed in water. Further experiments will be conducted to determine the heat flow when in SC\_11 nm is immersed in Aquivion dispersed in alcohol-water mixtures.

### 3.2 Improved cathode catalyst layer stability

Figure 6 highlights the ECSA and MA performance of PtCo/SC samples, both initially and after 30,000 AST cycles, in comparison to the project reference, JM Pt/C1. The PtCo/SC\_7 nm demonstrates an ECSA loss of only ~2 % after AST, while the PtCo/SC\_11 nm sample shows an ECSA loss of ~1 %. In contrast, the JM Pt/C1 reference exhibits a large ECSA loss of ~17 %. Despite the MA losses observed in the PtCo/SC samples (~52 % for PtCo/SC\_7 nm and ~40 % for PtCo/SC\_11 nm), they remained more active after AST than the reference catalyst, which decreased 46 %, their ability to maintain ECSA more effectively than the JM Pt/C1 sample underscores their superior stability in the cathode catalyst layer.

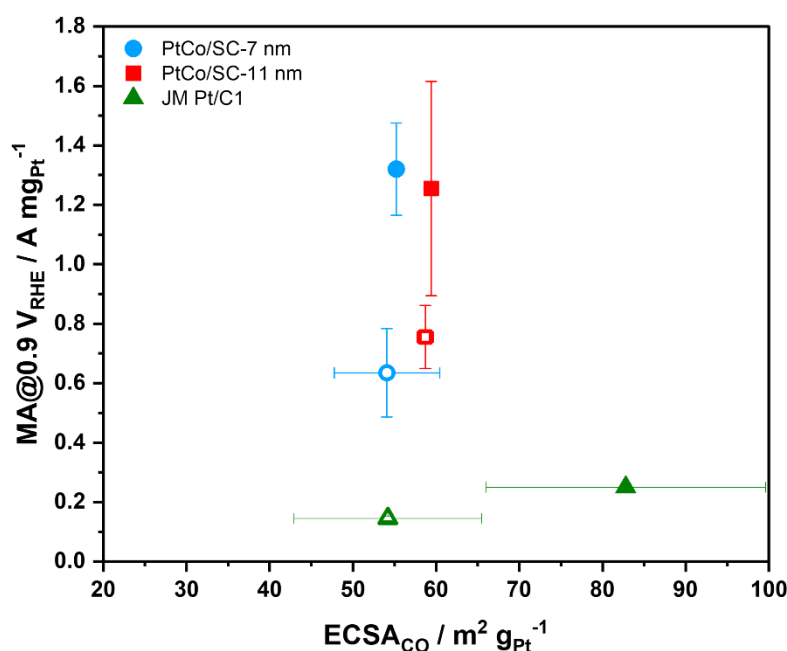


Figure 6: RDE result with mass activity MA at 0.9  $V_{RHE}$  versus  $ECSA_{CO}$  for PtCo/SC\_7 nm (blue circle), PtCo/SC\_11 nm (red square) and JM Pt/C1 (green triangle). Hollow symbols represent the data measured after AST. AST consisted of 30k trapezoidal cycles between 0.6  $V_{RHE}$  and 0.95  $V_{RHE}$ , 700  $mV s^{-1}$  sweeping rate with a holding time of 3 s in  $N_2$ -saturated 0.1 M  $HClO_4$  electrolyte.

## 4 CONCLUSIONS AND FUTURE WORK

With the aim of controlling ionomer coverage and catalyst dispersion in cathode catalyst layers, sulfur-functionalised carbon supports (CS) were developed in the frame of Highlander project. The interaction of such modified supports with PFSA ionomers and Pt-based nanoparticles was assessed using a range of characterisation techniques in comparison with reference electrocatalyst based on non-functionalised carbon black (Pt/C1).

XPS analysis of Pt 4f and S 2p regions revealed that PtCo/SC exhibit enhanced electronic interactions and stronger binding with Nafion than Pt/C1.

Immersion calorimetry was used to assess the interaction of bare carbon supports with water and Aquivion aqueous dispersions. The role of the heteroatom in enhancing the hydrophilicity of the carbon support was demonstrated. It appeared that higher sulfonic acid group content in the ionomer (lower EW) resulted in higher enthalpy of immersion, highlighting the role of sulfonic acid groups in the interaction with the support. To further understand the role of the presence of sulfur in the support on its interaction with ionomer, work is on progress to assess such interaction strength in conditions closer to actual inks, in the presence of mix of solvents at different ratios (water/alcohol).

RDE electrochemical characterisation demonstrated higher ECSA and mass activity retention upon AST for PtCo/SC, in alignment with improved ionomer stability, which will be further validated in a fuel cell.

## 5 REFERENCES

1. C.L. Yang, L.N. Wang, P. Yin, J. Liu, M.X. Chen, Q.Q. Yan, S.Z. Wang, S.L. Xu, S. Q. Chu, C. Cui, H. Ju, J. Zhu, Y. Lin, J. Shui, H.W. Liang, Sulfur-anchoring synthesis of platinum intermetallic nanoparticle catalysts for fuel cells, *Science* **2021**, 374, 459-464.
2. F. Yang, L. Xin, A. Uzunoglu, Y. Qiu, L. Stanciu, J. Ilavsky, W. Li, J. Xie, Investigation of the Interaction between Nafion Ionomer and Surface Functionalized Carbon Black Using Both Ultrasmall Angle X-ray Scattering and Cryo-TEM, *ACS Appl Mater Interfaces* **2017**, 9, 6530–6538.
3. A. Parnière, P.-Y. Blanchard, S. Cavaliere, N. Donzel, B. Prelot, J. Rozière, D.J. Jones, Nitrogen plasma modified carbons for PEMFC with increased interaction with catalyst and ionomer, *J. Electrochem. Soc.* **2022**, 169, 044502.
4. E. Hornberger, T. Merzdorf, H. Schmies, J. Hü, M. Klingenhof, U. Gernert, M. Kroschel, B. Anke, M. Lerch, J. Schmidt, A. Thomas, R. Chattot, I. Martens, J. Drnec, P. Strasser, Impact of Carbon N-Doping and Pyridinic-N Content on the Fuel Cell Performance and Durability of Carbon-Supported Pt Nanoparticle Catalysts, *ACS Appl. Mater. Interfaces* **2022**, 14, 18420–18430.